

CFD Simulation And Two-Phase Modeling Of A Non-Prismatic Converging Compound Channel

Abinash Mohanta¹, K. C. Patra², K. K. Khatua³

¹(Department of Civil Engineering, N.I.T Rourkela, Odisha
Email: abinash07552@gmail.com)

²(Department of Civil Engineering, N.I.T Rourkela, Odisha
Email: kcpatra@nitrkl.ac.in)

³(Department of Civil Engineering, N.I.T Rourkela, Odisha
Email: kkkhatua@nitrkl.ac.in)

ABSTRACT

Flooding situation in rivers is a complex phenomenon and affects the livelihood and economic condition of the region. The modeling of such flow is primary importance for a river engineers and scientists working in this field. A numerical investigation is carried out for studying different flow characteristics of a converging compound channel such as velocity distribution, depth averaged velocity distribution etc. The models using ANSYS – FLUENT are found to give satisfactory results when compared to the newly conducted experimental data under controlled system. Therefore, in this study an effort is made to analyze the turbulent structure by using Volume of fluid (VOF) two phase model and Large Eddy Simulation (LES) turbulence modeling to predict the flow characteristics of a non-prismatic compound channel. The LES is carried out by taking sufficient development length so that uniform turbulent flow is developed. However, it is a fact that numerical simulations of compound channels with different hydraulic conditions are computationally very expensive and arduous.

Keywords – CFD simulation, LES modeling, Non-prismatic compound channel, Two phase modeling, VOF model.

I. Introduction

Rivers have fascinated scientists and engineers. It is the main source of providing water supply for domestic, irrigation, industrial consumption or transportation and recreation uses. However, the design and organizing these systems require a full perception of mechanics of the flow and sediment in rivers. River channels do not remain straight for any appreciable distance. Flow separation in open channel expansion has been identified as one of the major problems encountered in many hydraulic structures such as irrigation networks, bridges, flumes, aqueducts, power tunnels and siphons. Due to the existence of secondary flow, flow characteristics in channel bends are much more complicated than those in straight channels. In other words, close to the inner wall and also at the channel bed, pressure gradient exceeds centrifugal force and conveys water in a transverse direction towards the inner wall. At the free surface, centrifugal force drives the flow to the outer wall. This kind of flow is known as the secondary flow [1]. During this process, energy losses taken place due to changing flow condition in the channel compression. Moreover, the presence of adverse pressure gradient causes flow separation due to the inability of flow to adhere to the boundaries and losses of head taken place due to

subsequent formation of eddies. So to reduce bed and bank erosion, control of flow separation is required. The basic principle in the application of CFD is to analyze fluid flow in-detail by solving a system of non-linear governing equations over the region of interest, after applying specified boundary conditions. A step has been taken to do numerical analysis on a non-prismatic compound channel flow having converging floodplains. The work will help to simulate the different flow variables in such type of complex flow geometry.

In the present work, an effort has been made to investigate the velocity profiles for three different sections of a compound channel having converging flood plain by using a computational fluid dynamics (CFD) modeling. The CFD model developed for a real open-channel is first validated by comparing the velocity profile obtained by the numerical simulation with the actual measurement carried out by experimentation in the same channel using pitot tube. Earlier a few experiments were carried out related to this field and various methods were investigated the suppress flow separation [2] [3]. To investigate complex flow characteristics of compound open channel expansion some recent flow measurements techniques and digital technology like Laser Doppler Anemometry (LDA) are created. Now a days

computational or numerical method are adopted for this type of case study. By using large eddy simulation (LES) method the flow pattern at a curved channel [4] and a curved 180° bend channel [5] are modeled and assessed the secondary flow structure. By using the standard k-e turbulence model a three dimensional numerical model was investigated to simulate the secondary flows, bed shear stress distribution, the longitudinal and transversal changes of water depth and the distribution of velocity components at bend [6] [7]. In [8], author determined the velocity profiles in both the directions under different real flow field conditions and also investigated the effects of bed slope, upstream bend and a convergence/divergence of channel width [8]. To study the negatively buoyant flow in a diverging channel with sloping bottom k-e turbulence model used and analyzed the effect buoyant effect [9]. By simulating the Computational fluid dynamics (CFD) software with fluid flow interactions between phases a experimentation of multiphase flow was improved to analysis and compare the results on flow regime and pressure drop within a flow regime [10]. The three-dimensional flow pattern in a sharp bend was simulated by using two different numerical codes along with different turbulent models and by comparing the numerical results with experimental results stated about the relevance of RSM turbulence model [11]. From all turbulence model, LES model are resolve large eddies directly, whereas small eddies are modeled. However, LES models generally require much denser grids [12]. Including all these studies some other studies on non-prismatic compound channel and converging flood plain have also been conducted by researchers [e.g. Salami [13], Knight and Shiono [14], Feng [15], Bousmar [16], Nezu [17], Proust [18], Razaei and Knight [19], Baghalian [20] and Liu [21]. The simulated flow field in each case is compared with corresponding laboratory measurements of velocity and water surface elevation.

II. Experimental Setup and Measurements

Experiments was conducted in non-prismatic compound channels having symmetrically converging flood plains with varying cross section built inside a concrete flume measuring 15m×.9m×0.5m at National Institute of Technology Rourkela Hydraulic laboratory. The width ratio of the channel is $\alpha \leq 1.8$ and the aspect ratio is $\delta \geq 5$. The converging angle of the channel is 13.39°. Converging length of the channel is 0.84m. The channel is made up of cement concrete. Fig.1 shows the schematic diagram of experimental setup of the open channel flow. Fig.2 shows the plan

view of three different experimental sections of a converging compound channel. The parameters of the channel are aspect ratio of main channel (δ), width ratio (α). Experimentation is taken place in the compound channel by taking different relative depth (Dr) value i.e. 0.5Dr, 0.2Dr, 0.3Dr in different position and depth. In this paper experimentally calculated results of 0.3Dr value is taken for analysis with numerical analysis results of various depth and position longitudinally in three different sections. Where first section is taken before start of converging area, second section is taken in middle of converging area and third section is taken after the end of converging area. In Fig 2 it is clearly shown that only section 2 is situated in between converging area whereas section 1 and 3 is situated outside the converging area. In section 1 width ratio (α) is more (1.8) where in section 3 width ratio is less=1 as there is no flood plain. It means after section 1 flood plain converges towards longitudinal direction. The detail descriptions of experimentation are given in Table 1.

Table 1: Description of Compound Channel

Sl No	Item Description	Converging Compound channel
1	Geometry of main channel	Rectangular Type
2	Geometry of flood plain	Converging Type
3	Relative Depth(Dr)	0.3
4	Width Ratio(α)	$1 \leq \alpha \leq 1.8$
5	Aspect Ratio(δ)	5
6	Converging Angle	13.39°
7	Position of section 1	0.05m backward from start of convergence.
8	Position of section 2	0.47m forward longitudinally from section 1.
9	Position of section 3	0.89m forward longitudinally from sec 1 or 0.05 m forward from end of convergence.

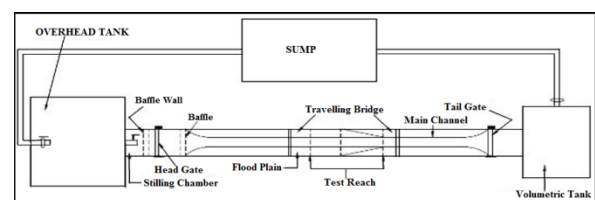


Fig1. Plan view of experimental setup of the channel

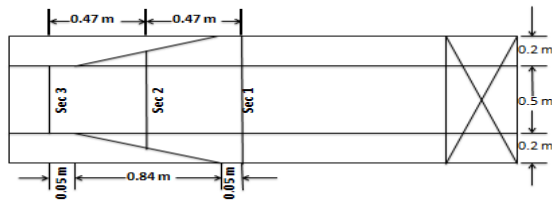


Fig 2: Plan view of three different experimental sections

III. Description of Numerical Model Parameters

Numerical codes used in this study (Fluent) are based on the full three-dimensional form of Navier-Stokes equations, and it uses a finite volume method (FVM). Fluent can use both structured and unstructured grids. For the solution that requires transient simulation, such as free-surface modeling e.g., VOF [22] model and the large Eddy Simulation (LES) turbulence modeling, the governing equations are discretized in both space and time. The algorithms adopted to solve the coupling between pressure and velocity fields in the Navier-Stokes equations in this study was pressure implicit with splitting of operators (PISO) for the numerical analysis [23]. PISO is a non-iterative solution method to calculate the transient problem, which converges faster [23]. The numerical solution requires criteria for determining the convergence of the acquired solution in iteration process. The numerical solution was converged when the residuals of the discretized equation reached a value of 0.001, or when the solution did not change with further iterations.

3.1 Governing Equations

The governing equations for the present study are the equations of conservation of mass, momentum and energy. The equation used for conservation of mass (the continuity equation) may be written as:

$$\frac{\partial \rho}{\partial t} + \rho \frac{\partial U_i}{\partial x_i} = S_m \quad (1)$$

The source term S_m contains the mass added through phase changes or user defined sources. In general, and in the simulations described here, the source term was equal to zero.

3.2 Turbulence Modeling

Turbulent flows have wide range of length and time scales. The large scale motions are generally energetic than the small ones and their size makes them the most effective transporters. Large eddies depend highly on boundary conditions which determine the basic feature of flow. Large scale eddy helps in transfer of momentum and heat. This technique directly resolves the large eddies present in

turbulent flows and models the smaller scale eddies. LES models are based on filtering the spectrum of turbulent eddies in the Navier–Stokes equations. The filter is related to grid size, and is usually chosen to be the actual grid size. Eddies smaller than the grid sizes are thus removed and must be modeled by a subgrid scale (SGS) model. Larger eddies are directly solved by the filtered transient Navier–Stokes equation:

$$\frac{\partial \overline{u_i}}{\partial t} = \frac{\partial \overline{u_i u_j}}{\partial x_j} = \frac{1}{\rho} \frac{\partial \overline{\sigma}}{\partial x_i} + \frac{\partial}{\partial x_i} \left(\overline{\theta} \frac{\partial \overline{u_i}}{\partial x_j} \right) - \frac{\partial \tau_{ij}}{\partial x_j} \quad (2)$$

Where τ_{ij} is the subgrid scale turbulent stress, which must be modeled. For our simulations, I chose the Smagorinsky–Lilly model which was the standard one available in Fluent. We also tried the WALE model on a test case with no difference in the results.

3.3 Geometry Domain and Boundary condition

For a given computational domain, boundary conditions are imposed which can sometimes over specify or under-specify the results of experimentation. Usually, after imposing boundary conditions in a non-physical domain, it's may lead to failure of the solution. The boundary conditions implemented for this study are shown in Fig-3. The channel analysed here allows the values on the inlet and outlet boundaries to coincide and a pressure gradient was further specified across the domain to drive the flow. A mean velocity was specified over the whole inlet plane to initialize the flow upon which velocity fluctuations were imposed. The inlet mean velocities were derived from the experimental average values. In order to specify the pressure gradient the channel geometries were all created with 0.0017 channel bed slopping and the effects of gravity and channel slope implemented via a resolved gravity vector. It represents the angle between the channel slope and the horizontal, the gravity vector is resolved in x, y and z components as

$$\rho g = (\rho g \sin \theta, 0, -\rho g \cos \theta)$$

Where θ = angle between bed surface to horizontal axis. Here, the x-component denotes the direction responsible for flow of water along the channel and the z-component is responsible for creating the hydrostatic pressure. From the simulation, z-component of the gravity vector ($\rho g \sin \theta$) is found to be responsible for the convergence problem of the solver. A no-slip boundary condition is the most common boundary condition implemented at the wall and prescribes that the fluid next to the wall assumes the velocity at the wall, which is zero.

$$U = V = W = 0$$

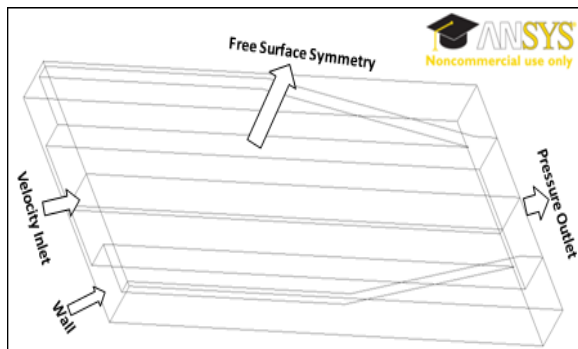


Fig 3: A Schematic diagram of compound channel with Boundary Condition

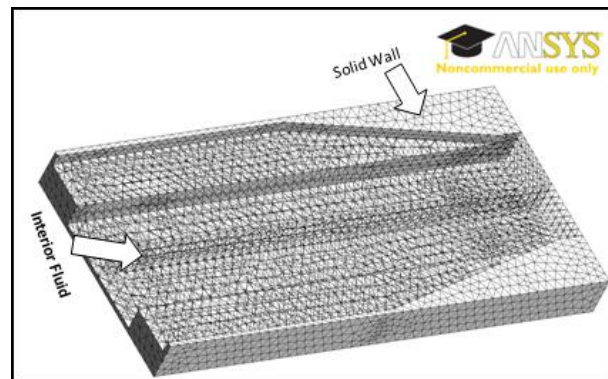


Fig 5: Meshing of compound channel

3.4 Grid Generation

It must be noted that the grid-independent results are obtained and the running time is low. The grid structure must be fine enough, especially near the wall boundaries (in order to consider the viscous flow), in the bend (the rapid changes area) and free surface. In this numerical model, various computational trials are conducted with different number of grid cells in x, y and z directions. It was concluded that the results are almost independent from the grid size and running time is optimal. The fluid flow governing equations (momentum equation, continuity equation) are solved based on the discretization of domain using the cartesian coordinate system. The CFD computations need a spatial discretization scheme and time marching scheme. This method is suitable with respect to both structured and unstructured mesh. At the mesh construction stage, it is decided to model only the half section of the channel and exploit the symmetry in the unsteady state flow as shown in Fig.4. Thus a symmetry condition is applied along the boundary at the centre of the channel. The meshing of the compound channel is shown in Fig.5.

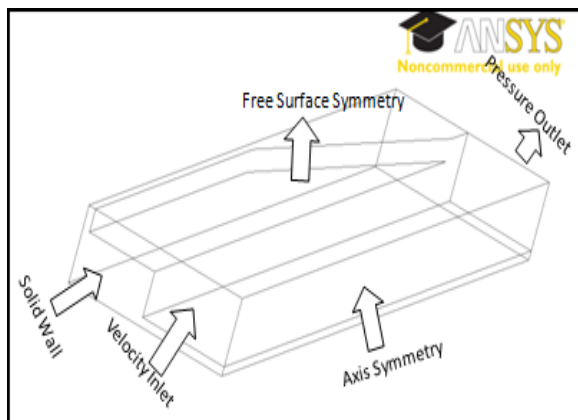


Fig 4: Half Sectional Compound channel with Symmetry condition

IV. Result and Discussion

In this study, various flow variables were studied in a converging compound channel with three different sections, which are discussed separately below. The positions of different experimental three sections are clearly shown in Fig 6. To see the effect of turbulence and boundary shear and to compare these effects two sections are taken outside the converging part. One is (section 1) which is situated before the converging part and other section is taken after the converging part (section 3). Other section (section 2) is taken inside the convergence area. To compare the effect of convergence and to analyse the secondary flow structure in between the channel velocity is measured in different positions experimentally by using pitot tube. In the experiments, the local velocities were measured at nodes located in different depths and widths in each section. As flood plain width is decreases gradually the vertical distributions of the velocity with the logarithmic law are shown in Fig 7 to 9 for validation of experimental results with CFD numerical analysis in three different sections accordingly. The results showed that the velocity gradient at interface zone decreased by taking $Dr=0.3$. Toward a longitudinal direction in a non-prismatic shape, in a constant Dr results decrease in the velocity gradient at interface zone. In all of the tests, the velocity gradient after the end of convergence reach was much higher than the other reach in a non-prismatic channel. Lateral depth-averaged velocity distributions were calculated and compared with the CFD results which are shown in Fig 10, Fig 11, Fig 12 for section 1, section 2 and section 3 respectively. As shown in this figure, in the non-prismatic compound channel with the same angle of convergence, increasing the aspect ratio or decreasing the width ratio led to an increase in the difference between the mean velocity in the main channel and floodplain. Along the compression of the flood plain of the channel by the expansion of the major and minor secondary flows, it can be seen that in sections 3(middle of convergence) contours of the

longitudinal velocity shift and the high velocity zone moves further towards the outer wall and along the channel convergence. And at the section after the bend (section 3), the high velocity zone is completely separated from the symmetry axis and transferred to the outer wall and the channel bed. The comparison of velocity contour between experimental data and numerical analysis of different sections are shown in Fig 13, Fig 14, Fig 15 respectively. Fig 13(a), Fig 14(a), 15(a) is shown the velocity contour of section 1, 2, 3 respectively by CFD software named as ANSYS Fluent. And Fig 13(b), Fig 14(b), Fig 15(b) is shown the velocity contour of different section from 1-3 respectively by experimental data using the software named as SURFER.

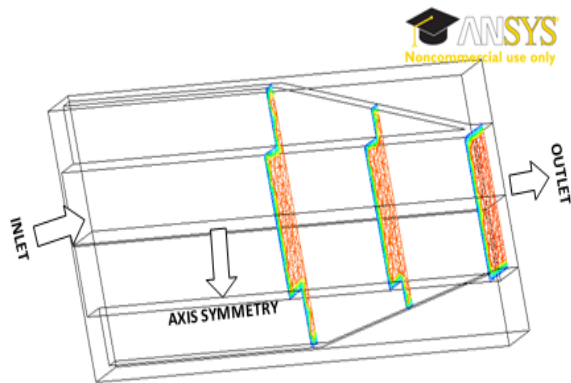


Fig 6: Positions of three different experimental sections

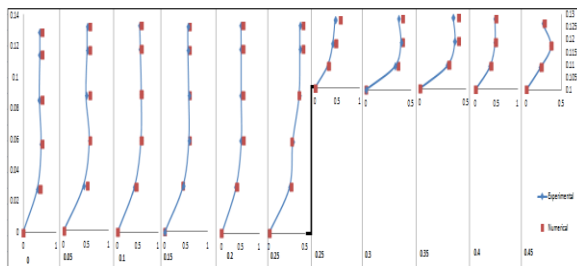


Fig 7: Distribution of the longitudinal velocity component at Section 1

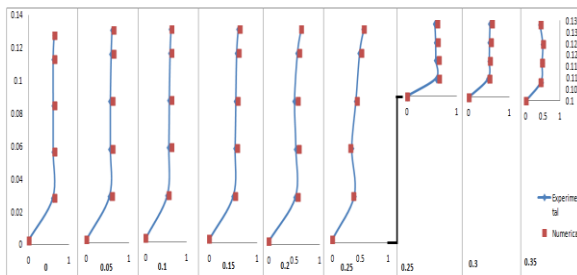


Fig 8: Distribution of the longitudinal velocity component at Section 2

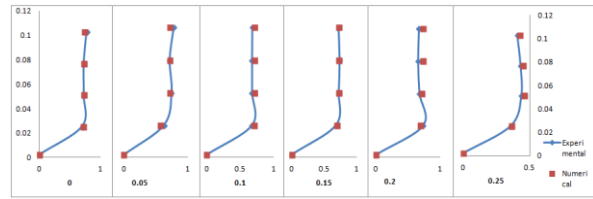


Fig 9: Distribution of the longitudinal velocity component at Section 3

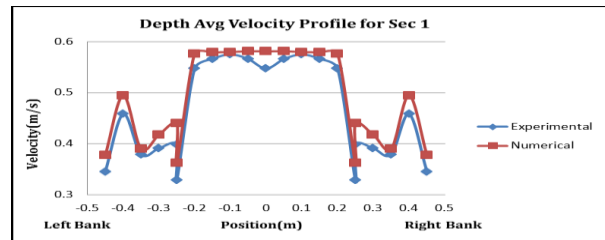


Fig 10: Depth Avg. Velocity profile of Sec 1

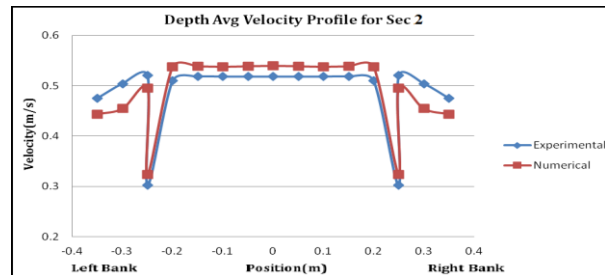


Fig 11: Depth Avg. Velocity profile of Sec 2

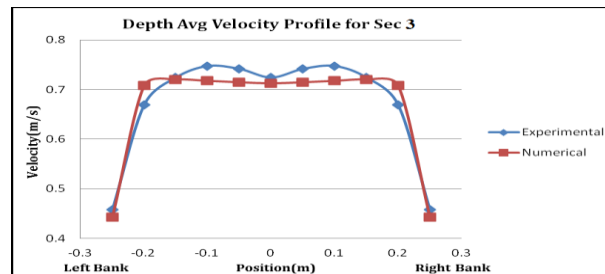


Fig 12: Depth Avg Velocity profile of Sec 3

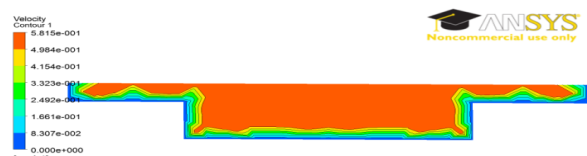


Fig 13(a): Velocity Contour of Sec 1 by Numerical analysis

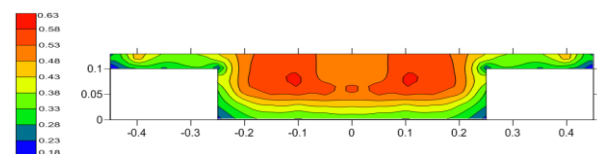


Fig.13(b) Velocity Contour of Sec 1 by Experimental Data

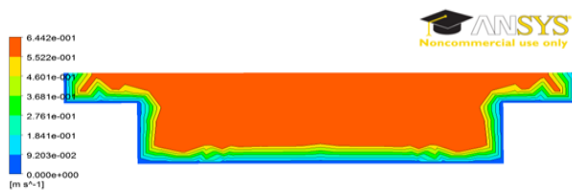


Fig.14(a). Velocity Contour of Sec 2 by Numerical analysis

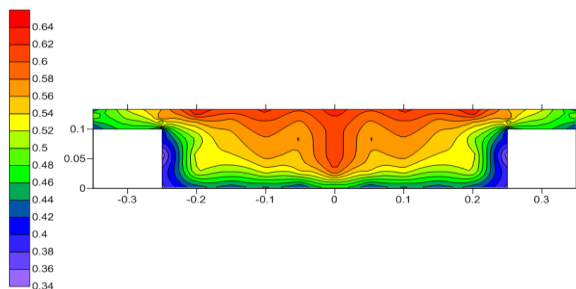


Fig.14(b). Velocity Contour of Sec 2 by Experimental Data

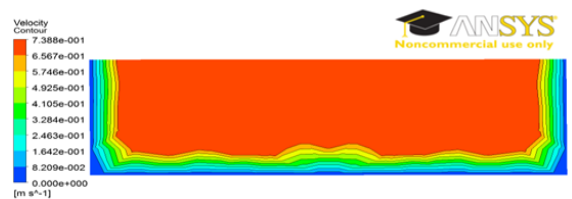


Fig.15(a). Velocity Contour of Sec 3 by Numerical analysis

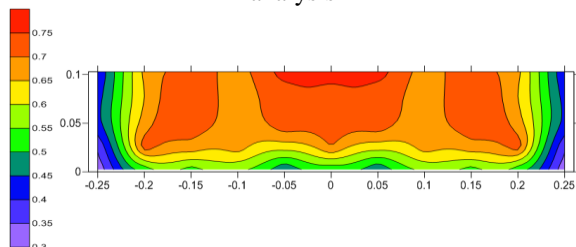


Fig 15(b): Velocity Contour of Sec 3 by Experimental Data

V. Conclusion

A complete three-dimensional two phase CFD model with finite volume method (FVM) and a dynamic Sub grid-scale for prediction of flow distribution in a non-prismatic compound channel is investigated. Here experimental velocities are compared with the velocities obtained from Numerical analysis of sec-1, sec-2, sec-3 of the channel. On the basis of velocity contour it is concluded that there is a good agreement between the results of the CFD analysis and the experimental data. The variation of longitudinal velocity in main channel region is found to be less as compared to that in the flood plain region. In main channel region the velocity magnitude is nearly constant after the solid

boundary however at flood plain region there is rapid variation found and maximum velocity occurs just below the free surface. From depth-average velocity profile, it clearly conclude that at section1 the numerical analysis gives good results and it is slightly overestimating the data when it is compared with the experimental result with an positive error of more or less than 5% but when the numerical analysis results are compared with the rest of the section, then it is underestimating the data. As width ratio of the channel goes on decreasing from sec 1 to sec 3, the results obtain from the numerical analysis also goes on underestimating when it is compared with the experimental results whereas at sec-2, the numerically estimated velocity results underestimate the experimental datas at floodplain whereas at main channel the numerically estimated results overestimate the experimental results. So the net discharge at sec-2 remains same for both the case. But at sec-3, the numerically estimated results underestimate the results obtain from experimentation with the negative error of more or less than 5% of error.

REFERENCES

- [1] H. Lien, "Bend-Flow Simulation Using 2D Depth-Averaged Model", *Journal of Hydraulic Engineering*, 125(10), 1999, 1097-1108.
- [2] R.S. Chaturvedi, "Expansive sub-critical flow in open channel transitions", *Civil Engineering Division*, 43, 1962, 447.
- [3] C.D. Smith, N.G. Yu, "Use of baffles in open channels expansion", *Journal of The Hydraulic Div., ASCE, HY2*, 1966, 1-17.
- [4] R.Booij, "Measurements and large eddy simulations of the flows in some curved flumes", *J. Turbul*, 4(8), 2003, 1-17.
- [5] W.VanBalén, W.S.J.Uijtewaald, K. Blanckaert, "Large-eddy simulation of a mildly curved open-channel flow", *Journal of Fluid Mechanics*, 630(1), 2009, 413-442.
- [6] T. Bodnar, Prihoda, "Numerical simulation of turbulent free-surface flow in curved channel Flow", *turbulence and combustion*, 76(4), 2006, 429-442.
- [7] O. Seyedashraf, Ali Akbar, M.K. Shahidi, "Numerical Study of Channel Convergence Effects on Flow Pattern in 90 Degree Bends", *9th International Congress on Civil Engineering*, Isfahan University of Technology (IUT), Isfahan, Iran, 2012, 1-8.
- [8] B.K.Gandhi, H.K.Verma, B.Abraham, "Investigation of Flow Profile in Open Channels using CFD", *IGHEM*, 2010, 1-12.
- [9] Z.Ahmad, U.C. Kothiyari, K.G. Ranga Raju, "Longitudinal dispersion in open channels",

- ISH Journal of Hydraulic Engineering*, 5(2), 1999, 1-21.
- [10] A.G. Dixon, G. Walls, H. Stannes, M. Nijemeisland, E.H. Stitt, "Experimental validation of high Reynolds number CFD simulations of heat transfer in a pilot-scale fixed bed tube", *Chemical Engineering Journal*, 200-202(0), 2012, 344-356.
- [11] A.Ramamurthy, S.Han, P.Biron, "Three-Dimensional Simulation Parameters for 90° Open Channel Bend Flows", *Journal of Computing in Civil Engineering*, 27(3), 2013, 282-291.
- [12] W.VanBalen, K.Blanckaert, W.S.J. Uijtewaal, "Analysis of the role of turbulence in curved open-channel flow at different water depths by means of experiments LES and RANS", *Journal of Turbulence*, 12, 2010.
- [13] L.A Salami, "On velocity-area methods for asymmetric profiles", University of Southampton Interim Report V, 1972.
- [14] D.W.Knight, K.Shiono, "Turbulence measurements in a shear layer region of a compound channel", *Journal of Hydraulic Research*, 28(2), 1990, 175-196.
- [15] K.Shiono, T.Feng, "Turbulence measurements of Dye Concentration and Effects of Secondary Flow on Distribution in Open Channel Flows", *Journal of Hydraulic Engineering*, 129(5), 2003, 373-384.
- [16] D.Bousmar, N. Wilkin, J.-H. Jacquemart, Y. Zech, "Overbank Flow in Symmetrically Narrowing Floodplains", *Journal of Hydraulic Engineering*, 130(4), 2004, 305-312.
- [17] I. Nezu, "Open-Channel Flow Turbulence and Its Research Prospect in the 21st Century", *Journal of Hydraulic Engineering*, 131(4), 2005, 229-246.
- [18] S. Proust, N. Riviera, D. Bousmar, A. Paquier, Y. Zech, R. Moral, "Flow in Compound Channel with Abrupt Floodplain Contraction", *Journal of Hydraulic Engineering*, 132(9), 2006, 958-970.
- [19] B.Rezaei, D.W.Knight, "Application of the Shiono and Knight Method in compound channels with non-prismatic floodplains", *Journal of Hydraulic Research*, 47(6), 2009, 716-726.
- [20] S.Baghalian, H.Bonakdari, M.Fazli, "Numerical simulation of flow in open channel with a 90° bend", *6th National Congress on Civil Engg., Iran*, 2011, 1-8.
- [21] T.H.Liu, Li Chen, B.L.Fan, "Experimental study on flow pattern and sediment transportation at a 90° open-channel confluence", *International Journal of Sediment Research*, 27(2), 2012, 178-187.
- [22] J.H.Ferziger, M.Peric, "Computational methods for fluid mechanics", *Springer*, 2002, 85-127.
- [23] R.I.Issa, "Solution of the implicitly discretised fluid flow equations by operator-splitting", *Journal of computational physics*, 62(1), 1986, 40-65.